

Born for Auto-Tagging: Faster and better with new objective functions^{*}

Chiung-ju Liu¹ and Huang-Ting Shieh¹

awoo Intelligence AI
{cjliu, timshieh}@awoo.ai

Abstract. Keyword extraction is a task of text mining. It is crucial to increase search volume in SEO and ads. Implemented in auto-tagging, it makes the process on a mass scale of online articles and photos efficiently and accurately. BAT was invented for auto-tagging, serving as awoo’s AI marketing platform (AMP). It not only provides service as a customized recommender system but also increases the converting rate in E-commerce. The strength of BAT converges faster and better than other SOTA models, as its 4-layer structure achieves the best F scores at 50 epochs. In other words, it performs superior to other models which require deeper layers at 100 epochs. To generate rich and clean tags, we create new objective functions to simultaneously maintain similar F_1 scores with cross-entropy while enhancing F_2 scores. To assure the even better performance of F scores, we revamp the learning rate strategy proposed by Transformer [17] to increase F_1 and F_2 scores at the same time.

Keywords: Text classification · objective functions · contrastive learning.

1 Introduction

Keywords are widely used for site search, ads, and personalized recommendations on E-commerce, news sites, streaming media, etc. In particular, keyword search dominates the performance in search engine optimization (SEO). Valuable words such as high search volume are used to write articles with strong content or target popular issues. Automatically keyword extraction is helpful in online business.

Keyword extraction is essential in text mining, information retrieval, and natural language processing (NLP). However, it is challenging when it is implemented on web data or industry documents. The difficulty is not only due to the scale of data but also noisy signals including unstructured sentences, emotional symbols, network language, etc. Manual labeling for keywords is time-consuming. The consistency of labeling differs from labelers and needs rules to supervise. Machine learning emerges to solve the problem. Unsupervised algorithms based on statistic models are known as TF-IDF, BM25, and YAKE [1]. Graph-based models include TextRank [9], Rake [12], Singlerank [18] etc. Supervised learning with neural networks has had various developments recently. Some approaches are based on ranking the matching scores of queries with documents [6,20,19,10]. Others are performed as semantic analysis classification [21,16], etc.

awoo is successful in utilizing valuable tags in E-commerce, retail stores, AdTech, SEO, retargeting service, and business intelligence. awoo AMP uses tags to help customers to find products efficiently and increase conversion rates. Tagging for product pages not only advantage in keyword search but also benefits online stores in managing products.

^{*} We thank Tung-Chi Tsai and Liang-Wei Liu for the technical support and discussion during the preparation of the paper.

Most personal recommendation systems are based on collaborative filtering. It focuses either on items that one bought in the past or other people bought in common. However, personal interest shifts or relating to popular items may cause poor recommendations. Understanding products and focusing on the message of the items by tags may capture customers' intentions. We use A/B test to show that it increases 71% search volume, 230% time on page, 200% conversion rates, and 100% per customer transaction on average. It does induce great shopping serendipity.

To generate tags for large E-commerce platforms, we investigate extracting tags automatically. Tags range over categories, goods, brands, and features, varying in different industries. They are complicated and technical to establish rules. However, we have extensive experience in managing tags due to our long-term business in SEO.

BAT (**B**orn for **A**uto-**T**agging) is reconstructed from the encoder of Evolved Transformer [14]. This model is created for auto-tagging. It converges faster and better than other SOTA models. Its 4-layer structure (figure 3) obtains the best F scores at 50 epochs and the scores exceed the other deep layers at 100 epochs. To generate rich (higher F_2) and clean (higher F_1) tags, we create new objective functions L_{PBP} (9) and L_{CECLA} (7) to maintain similar F_1 scores with cross-entropy L_{CE} but also increase F_2 scores simultaneously. See figure 1 and 2 for detail.

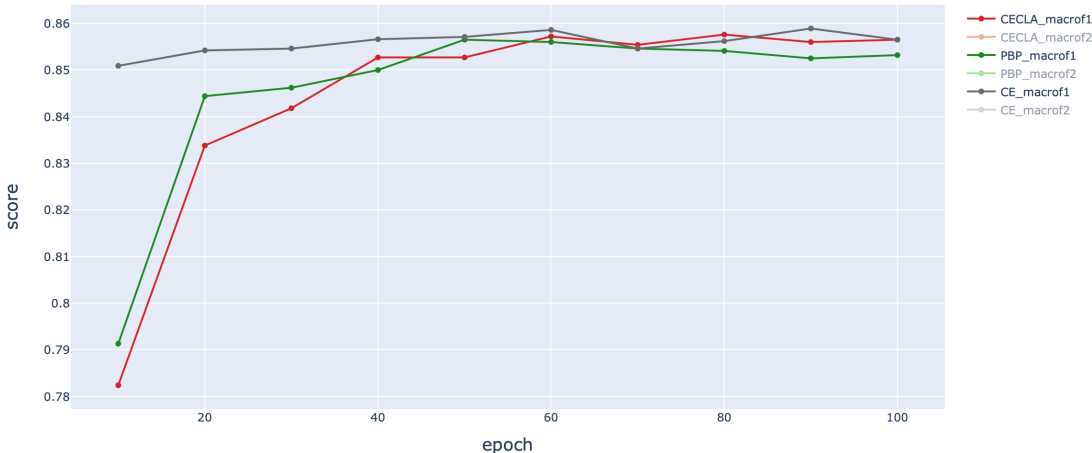


Fig. 1. Loss comparison of CECLA, PBP, and CE with F_1 scores

Industry aspects such as SEO and ads value F_2 scores more than F_1 scores. On the other hand, security-related businesses such as fingerprint recognition or medical object

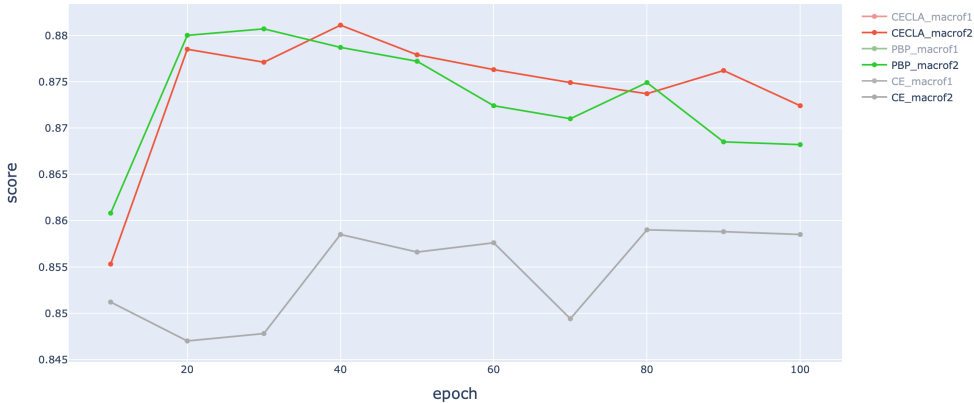


Fig. 2. Loss comparison of CECLA, PBP, and CE with F₂ scores

detection are concerned about precision or F₁ scores. Since we want to find not only plentiful but also neat tags, we look for the relative maximum of macro F₂ curves, not the lowest loss value. The optimal point may not occur at the end of the training by minimizing the loss. To overcome this problem and enhance a better convergence, we revamp the learning rate strategy (10) proposed by Transformer [17] to increase F₁ and F₂ scores at the same time. See table 1 for complete information.

In the classification task on EC-Zh data, BAT gets 1.7%, 3.1%, 3.3% and 2.7% more than Transformer via L_{CE} , L_{WCE} , L_{CECLA} , and L_{PBP} objective functions with respectively in macro F₁ at 50 epochs. BAT obtains 2.9%, 2.2%, 2.3% and 2.2% more than Transformer by L_{CE} , L_{WCE} , L_{CECLA} and L_{PBP} loss functions with respectively in macro F₂ on EC-Zh data. Most SOTA models maintain almost the same F₁ scores via new loss functions and gain 2% F₂ on average by comparing to L_{CE} . Moreover, on EC-JP dataset, BAT gets 1.4%, 2.5%, 3.5%, and 2.8% in macro F₁ via L_{CE} , L_{WCE} , L_{CECLA} and L_{PBP} with respectively. BAT gets 1.7%, 0.8%, 1.6%, and 1.5% in macro F₂ via L_{CE} , L_{WCE} , L_{CECLA} and L_{PBP} with respectively. See the experiment of comparison in section 5.2.

2 Related Work

2.1 Contrastive Learning

An objective function plays an important role in supervised learning. It directly LeCun etc. introduced the contrastive loss function in [5]. It is well known as triplet loss [13] in image classification. Given a pair $\{x_+, x_-\}$ of a positive and negative sample and a training sample x , the object is to make x look similar to x_+ and not similar to x_- if x is

labeled as positive ($y = 1$). The triplet loss is formulated as

$$L = \max(0, \|x - x_+\|^2 - \|x - x_-\|^2 + \alpha) \quad (1)$$

for binary classification. The model is supervised to learn to draw close to x_+ and push away from x_- with a marginal distance α . The feature space is measured in L_2 -norm. It is applied to multiple classification [15]. The $(N + 1)$ -tuple loss is to optimize identifying a positive sample from N negative samples. It is

$$L(x_i, x_j) = \mathbf{1}\{y_i = y_j\}\|x_i - x_j\|^2 + \mathbf{1}\{y_i \neq y_j\} \max(0, \alpha - \|x_i - x_j\|^2) \quad (2)$$

When $N = 2$, it is equivalent to triplet loss. Since it is not easy to train an NLP model by using L_2 -norm, we prefer to use cross-entropy in binary classification:

$$L = y \log p + (1 - y) \log(1 - p), \quad (3)$$

where $y = 1$ if x is positive and $y = 0$ if x is negative, and p is the prediction of x . For multiple classifications, we formulate it as equation 5. We discuss the objective functions exhaustively in section 4.1.

3 Model Architecture

BAT is a model reconstructed from Evolved Transformer’s architecture [14]. We use the encoder for text classification. The complete encoder-decoder structure is designed for machine translation and other tasks matching different input and output sequence lengths. Attention mechanisms in RNN models [2] integrate the total inference of the input sequence with each output which accelerates the development of progress in NLP. Transformer adopts full attention and exempts from sequential input which makes a leap of development in deep learning. It dominates machine learning in all aspects. Many models are developed from it.

3.1 Input

The encoder imports a sequence of tokens $\{w_1, \dots, w_n\}$ with vector embedding $\{\mathbf{x}_1, \dots, \mathbf{x}_n\}$ respectively. Since Transformer uses position encoding to replace the sequential input, the encoder can input the data $X = [\mathbf{x}_1, \dots, \mathbf{x}_n]^T \in \mathbb{R}^{n \times d_e}$ and output the probability $[\mathbf{p}_1, \dots, \mathbf{p}_n]^T \in \mathbb{R}^{n \times C}$ for each token at the same time.

Transformer [17] adds up the position encoding and embedding vectors to be the feature representation. One can change it to a linear or affine linear combination for richer inputs. GPT2 [11] moves the layer normalization (LN) before the self-attention block and obtains a better result. Admin [8] shows that Pre-LN maintains steady gradient distribution through each layer in the decoder but does not affect much in the encoder. We have an ablation experiment for a text classification task with a 4-layer encoder. Pre-LN obtains a slice better result.

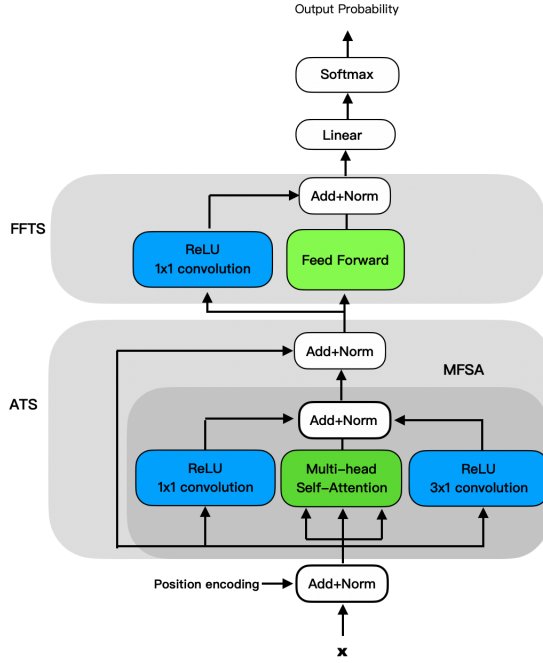


Fig. 3. Architecture of BAT

3.2 Encoder

The encoder is composed of a stack of identical layers (4 layers for commercial requirements). Each layer consists of two sublayers: attention and feed-forward tournament selection sublayers (ATS and FFTS). The competition forms differently: MFSA races with constant residual connection and FFNN races with a weighted residual connection. The two parallel branches compete through backpropagation to update parameters for better performance.

3.2.1 ATS: Attention Tournament Selection Sublayer ATS sublayer contains a multiple-feature self-attention block (MFSA) and a residual connection in parallel. Inspired by [14], we extract multiple features from the input: multi-head self-attention, 1×1 -convolution, and 3×1 -convolution in parallel. It can be formulated as

$$\text{MFSA} = f_{\text{LN}}(\text{MultiHead}(Q, K, V) + f_{1 \times 1 \text{conv}}(X) + f_{3 \times 1 \text{conv}}(X)). \quad (4)$$

3.2.2 MFSA: Multiple Feature Self-Attention MFSA Adds up Three Features:

- The Multi-head attention is directly followed from Transformer [17].

- The 1×1 -convolution followed by the activation ReLU captures the relation of oneself. The activation ReLU plays a role as a dropout.
- The 3×1 -convolution followed by the activation ReLU captures the relation between the current word with its context words. This represents a local feature.

3.2.3 FFTS: Feed-Forward Tournament Selection Sublayer FFTS is created for the competition between two branches: FFNN and weighted residual connection. An ablation experiment shows that FFNN needs support from weighted res-connection to achieve prosperity.

4 Training

Suppose that training data $\{(\mathbf{x}_i, \mathbf{y}_i)\}_{i=1}^N$ is a set of pairwise vectors, where $\mathbf{x}_i \in \mathbb{R}^{d_e}$ is the embedding of word w_i and $\mathbf{y}_i \in \mathbb{R}^C$ is its label. Labels are defined by humans.

4.1 Training Loss

An objective function affects the performance of an ML model crucially.

We create two types of objective functions for imbalanced data in multiple classification tasks.

- The CECL (categorical Cross-Entropy with Contrastive Learning) loss is given by

$$L_{\text{CECL}} = -(\mathbf{y} \log \mathbf{p} + (\mathbf{1} - \mathbf{y}) \log(\mathbf{1} - \mathbf{p})). \quad (5)$$

Given a sample with label $\mathbf{y} = [1, 0, 0]$, suppose that it has two two predictions $\mathbf{p}_1 = [0.4, 0.3, 0.3]$ and $\mathbf{p}_2 = [0.4, 0.5, 0.1]$. They obtain the same L_{CE} value but different

$$L_{\text{CECL}}(\mathbf{p}_1) = -\log(0.4) - \log(0.3) - \log(0.3) = 0.71$$

and

$$L_{\text{CECL}}(\mathbf{p}_2) = -\log(0.4) - \log(0.5) - \log(0.1) = 0.74.$$

The false prediction \mathbf{p}_2 obtains a larger loss value. It induces the model to learn more efficiently for a single token. Contrastive learning in L_2 -norm (1) separates the positive and negative samples with a certain margin. On the other hand, contrastive learning with cross-entropy does not reveal the physical meaning but the probability value that approaches the positive ($y = 1$) or negative samples ($y = 0$). See equation (13) and (14) as the point of view of gradients in Appendix A.

- The PBP (Punish Bad Prediction) loss is given as

$$L_{\text{PBP}} = -(\mathbf{y} \log \mathbf{p} + (\mathbf{1} - \mathbf{y}) \odot \hat{\mathbf{y}} \log(\mathbf{1} - \mathbf{p})), \quad (6)$$

where $\hat{\mathbf{y}}$ the predicted class of \mathbf{p} , which is a one-hot vector. L_{PBP} produces more loss value if the model predicts an incorrect category. In previous example, we get $L_{\text{PBP}}(\mathbf{p}_1) = -\log 0.4 = 0.4$ and $L_{\text{PBP}}(\mathbf{p}_2) = -\log 0.4 - \log 0.5 = 0.7$. It converges faster than L_{CE} and L_{CECL} .

4.2 Training Loss for Imbalanced Data

To implement L_{CECL} loss on imbalanced data for better performance on positive samples, we adapt weights α and β

$$L_{\text{WCECL}} = -\frac{1}{N} \sum_{i=1}^N \left(\alpha \mathbf{y}_i (\mathbf{1} - \mathbf{p}_i)^\gamma \log \mathbf{p}_i + \beta (\mathbf{1} - \mathbf{y}_i) \mathbf{p}_i^\gamma \log (\mathbf{1} - \mathbf{p}_i) \right). \quad (7)$$

By leveraging the positive and negative samples having equal expectations, we manipulate EE weights

$$\begin{cases} \alpha_{EE} = \left(\frac{N}{N_1}, \dots, \frac{N}{N_C} \right) \\ \beta_{EE} = \left(\frac{N}{(N-N_1)}, \dots, \frac{N}{(N-N_C)} \right) \end{cases}, \quad (8)$$

where N_1, N_2, \dots, N_C denote the number of samples of each category, and C denotes the number of categories.

To produce specific weights according to their category amounts of negative samples, we create array weights:

$$A = (A_{ij}) = \begin{cases} \frac{N}{N_i} & \text{if } i = j \\ \frac{N}{(C-1)N_j} & \text{if } i \neq j \end{cases}.$$

The CECLA (Cross-Entropy by Contrastive Learning with Array weight) loss is given as L_{CECLA} for $\alpha_i = A \mathbf{y}_i$ and $\beta_i = A \mathbf{y}_i$ in (7). In particular, $A \mathbf{y}_i$ extracts the j -th column of A if \mathbf{y}_i is in class j . L_{CECLA} induces fast convergence. It obtains its optimal (macro $F_1 = 85.7$ and $F_2 = 88.1$) with learning rate $\alpha = 7/15$, $\beta = -1/30$, and $\lambda = 1.001$ in (11) at 40 epochs. It increases accuracy not only for BAT but also for other SOTA models.

L_{PBP} with balanced weights is given by

$$L_{\text{PBP}} = -\frac{1}{N} \sum_{i=1}^N \left(\alpha \mathbf{y}_i (\mathbf{1} - \mathbf{p}_i)^\gamma \log \mathbf{p}_i + \beta ((\mathbf{1} - \mathbf{y}) \odot \hat{\mathbf{y}}) \mathbf{p}_i^\gamma \log (\mathbf{1} - \mathbf{p}_i) \right), \quad (9)$$

where $\mathbf{y}_i, \mathbf{p}_i, \hat{\mathbf{y}}, \alpha, \beta \in \mathbb{R}^C$. BAT obtains macro $F_1 = 85.5$ and $F_2 = 88.0$ with $L_{\text{PBP}_{1,8}}$ at 30 epochs for a learning rate $\alpha = 6/11$ and $\lambda = 0.999$ in (11). L_{PBP} indeed saves training costs.

4.3 Learning Rate Strategy

Transformer adapts the learning rate according to the following formula [17]:

$$\text{rate} = d_{\text{model}}^{-0.5} \cdot \min(\text{step_num}^{-1/2}, \text{step_num} \cdot \text{warmup_steps}^{-1.5}), \quad (10)$$

with $\text{warmup_step} = 4000$. To change the convergence of the learning, we adjust the learning rate.

Let $x = \text{step_num}$ and $S = \text{warmup_steps}$. Given $\alpha > 0$, we adjust the learning rate

$$\text{rate} = \lambda \cdot d_{\text{model}}^{-1/2} \cdot \min(S^\beta \cdot x^{-\alpha}, S^{-3/2} \cdot x), \quad (11)$$

by finding a β to satisfy the continuous property

$$S^\beta \cdot x^{-\alpha} = S^{-3/2} \cdot x.$$

In general, a smaller learning rate induces a slower and finer convergence. A relative larger α in (11) leads to faster convergence and higher F_1 scores. Here are some examples for $L_{CECLA_{1,20}}$ at 50 epochs.

lr	v1	v2	v3	v3.1	v4.1	v5
F_1	85.3	85.5	85.6	85.3	85.4	85.0
F_2	87.8	87.7	87.6	88.1	87.9	87.3

Table 1. Learning Rate Comparison

v1 represents the original learning rate (10). v2 represents $\alpha = 6/11$, $\beta = 1/22$. v3 represents $\alpha = 6/13$, $\beta = -1/22$ and v3.1 represents $v3 * 0.999$. v4 represents $\alpha = 7/15$, $\beta = -1/30$ and v4.1 represents for $v4 * 1.001$. v5 represents $\alpha = 11/20$, $\beta = 1/20$.

Roughly speaking, v2 converges slower than v1 due to the learning rate power of $\frac{6}{11} < \frac{1}{2}$. On the other hand, v3 converges faster than v1. v3 at 50 epochs is almost the same as v1 at 60 epochs. v3 * 0.999 converges slower than v3 and has higher F_2 scores. Although v4 converges slower than v1, v4 * 1.001 converges faster than itself. v4 * 1.001 obtains its optimal at 40 epochs with macro $F_1 = 85.7$ and $F_2 = 88.1$. Although v5 does not perform well at 50 epochs, It obtains its optimal at 40 epochs with macro $F_1 = 85.5$ and $F_2 = 88.1$.

Each model suits a different learning rate due to its amount of parameters and architecture.

5 Experiments

5.1 Training Data

We have two training datasets. The EC dataset contains product pages which consist of titles and descriptions. We clean the data with a list of regulations and stop words.

1. EC-Zh, which is collected from 5 E-commerce platforms, includes cosmetics, furniture, fashion, shoes, and large retail store. Product pages are written in traditional Chinese and writing styles vary from platform to platform. It contains 2000 product pages from each platform and is divided into 80% for training and 20% for testing. The average length is 46.6 words per page and the longest page is 368 in the training set. This dataset has high variance and is challenging for text classification.
2. EC-JP, which is collected from 11 E-commerce platforms, includes fashion, interior decoration, farm produce, and multiple categories. Product pages are written in Japanese and have different writing styles. We remove page lengths over 400 due to the efficiency of model training. EC-JP is twice of EC-Zh. The average length is 30 words per page.

Due to the privacy policy of these two datasets, we are not able to release them to the public for free use. To verify the effectiveness of our model, we provide the sample code with CoNLL 2003 as the source.

5.2 Accuracy Comparison with SOTA

5.2.1 Hardware

- 1080 GPU has 8G memory and its operating system is Ubuntu18.04.
- 1080Ti GPU has 11G memory and its operating system is Ubuntu21.10.

The framework deployed on them depends on the official codes. MUSE, Admin, and Informer use PyTorch. Transformer, Switch, Performers, and BAT use TensorFlow. Further setup for each model will be mentioned in the additional appendix.

5.2.2 Optimizer All experiments are trained with optimizer Adam [7] with $\beta_1 = 0.9$, $\beta_2 = 0.98$, and $\epsilon = 10^{-9}$. We adapt the base learning rate (10) with `warmup_steps = 4000`.

5.2.3 Hyperparameters To maintain the efficiency and accuracy of the performance, we chose a relatively small model compared to Transformer. Here are the hyperparameters that we set for the architecture and experiments.

N	d_{model}	d_{ff}	h	d_k	d_v	p_{drop}	n
4	128	512	4	32	32	0	1.316 MM

Table 2. Variations in the BAT architecture

N represents the number of encoders and n represents the total number of parameters.

5.2.4 Comparison on EC-Zh First, we compare the performance of the model BAT with Transformer [17], Switch Transformer [4], Admin [8], MUSE [22], Performer [3], and Informer [23] in EC-Zh dataset with four loss functions. We use the official or open-source code from the third place for a fair comparison. We extract the encoder of these SOTA models and add a classification layer on top of it.

The distribution of EC-Zh dataset is $N_1 : N_2 : N_3 = 21.2 : 1.9 : 1$. All models are built with 4-layer, 4 heads, and no dropout. The following experiments are trained under the same conditions: learning rate strategy, batch=8, and 50 epochs. The accuracy comparison of macro F_1 and F_2 are displayed in table 3 and 4 with respectively.

loss \ Model	BAT	Admin	Switch	MUSE	Transformer	Performers	Informer
CE	85.7	84.5	82.1	84.2	84.0	83.9	84.6
WCE	85.5	84.5	79.6	81.2	82.9	83.0	80.8
PBP _{0,8}	85.6	84.0	79.1	84.0	82.9	82.7	81.2
CLA _{1,20}	85.3	84.3	75.0	83.7	82.4	82.1	80.9

Table 3. F_1 SOTA comparison on EC-Zh

BAT is a model that converges faster than other SOTA models for the overall performance. BAT obtains the best F scores at 50 epochs and is better than the deeper structure of other SOTA models at 100 epochs. CLA_{1,20} represents CECLA loss with focal factor $\gamma = 1$ and multiplication factor $\lambda = 20$ in (22). PBP_{0,8} stands for PBP loss with EE weight, focal factor $\gamma = 0$ and $\lambda = 8$ in (22).

loss\Model	BAT	Admin	Switch	MUSE	Transformer	Performers	Informer
CE	85.7	83.7	81.8	83.4	83.8	82.8	84.0
WCE	87.9	86.2	84.6	87.2	85.5	86.4	85.6
PBP _{0,8}	87.7	86.4	84.5	87.6	85.5	86.4	86.0
CLA _{1,20}	87.8	86.0	82.5	87.7	85.3	86.2	86.2

Table 4. F₂ SOTA comparison on EC-Zh

5.2.5 Comparison on EC-JP dataset The distribution in the EC-JP dataset is $N_1 : N_2 : N_3 = 9.57 : 1 : 1.01$. All models are built with 4-layer, 4 heads, and no dropout. The following experiments are all trained under the same conditions: Adam optimizer, learning rate strategy (10), and batch=8. Table 5 is the accuracy comparison of SOTA models on macro F₁. Table 6 shows the accuracy comparison of SOTA models on macro F₂.

loss\Model	BAT	Admin	MUSE	Transformer	Performers
CE	85.8	84.8	84.7	84.4	84.8
WCE	85.4	84.6	84.8	83.4	81.2
PBP _{0,8}	85.6	83.4	82.5	83.6	80.3
CLA _{1,20}	85.6	83.9	82.6	82.1	80.9

Table 5. F₁ SOTA comparison on EC-JP

loss\Model	BAT	Admin	MUSE	Transformer	Performers
CE	86.1	84.2	85.1	84.4	85.6
WCE	88.3	87.7	87.3	87.5	86.5
PBP _{0,8}	88.6	87.3	87.6	87.2	87.2
CLA _{1,20}	88.3	87.5	87.5	86.7	86.3

Table 6. F₂ SOTA comparison on EC-JP

We adopt the learning rate (10) by multiplying 0.93 for CE loss to slow down the convergence. For CECLA loss, we adopts $\alpha = 6/11$ and $\beta = 1/22$ for (11) to increase F₂ score. Since the data of EC-JP is twice of EC-Zh and contains more positive samples, most SOTA models have higher F scores on EC-JP.

5.2.6 Layers Comparison on EC-Zh Experiments are done with the same conditions: CLA_{1,20} loss function, batch = 8, 100 epochs. Increasing training time is concerned with the convergence of deeper layers. Table 7 demonstrates the comparison of macro F₁. Table 8 demonstrates the comparison of macro F₂.

Admin adds the initialization parameters and improves the performance in deeper layers. Switch and Performers maintain stable performance among different layers of models. MUSE especially has higher F₁ scores in 12 and 24-layer structures. BAT is less sufficient in deeper layers. Transformer does not converge in the 24-layer structure with several versions of the learning rate.

layer\Model	BAT	Admin	Switch	MUSE	Transformer	Performers	Informer
4-layer	85.7	83.9	79.1	84.4	83.0	82.7	82.8
6-layer	85.4	82.9	76.1	84.2	82.9	83.7	83.6
12-layer	85.5	83.6	80.2	85.4	82.1	82.9	83.4
24-layer	85.1	83.4	71.0	85.2	33.9	84.3	82.3

Table 7. F₁ layers comparison

layer\Model	BAT	Admin	Switch	MUSE	Transformer	Performers	Informer
4-layer	87.2	85.5	84.1	86.9	85.3	85.3	86.5
6-layer	87.1	85.5	82.7	86.7	84.2	85.3	86.4
12-layer	86.9	85.5	85.1	86.7	85.3	86.0	86.3
24-layer	87.4	86.2	78.3	86.2	37.1	87.0	86.5

Table 8. F₂ layers comparison

A Gradient of Loss Functions

A.1 Cross-Entropy with Contrastive Learning

The loss of weighted focal categorical cross-entropy with contrastive learning is given by

$$L_{\text{WFCECL}} = -\frac{1}{N} \sum_{i=1}^N (\alpha \mathbf{y}_i (\mathbf{1} - \mathbf{p}_i)^\gamma \log \mathbf{p}_i + \beta (\mathbf{1} - \mathbf{y}_i) \mathbf{p}_i^\gamma \log (\mathbf{1} - \mathbf{p}_i)), \quad (12)$$

where $\alpha, \beta, \mathbf{y}_i, \mathbf{p}_i \in \mathbb{R}^C$ and C is number of categories. If we calculate the gradient for a single token for which \mathbf{y} is in class c and $\alpha = \mathbf{1}$ and $\beta = \mathbf{1}$, then we get

$$\frac{\partial L}{\partial p_c} = \gamma (1 - p_c)^{\gamma-1} \log p_c - \frac{(1 - p_c)^\gamma}{p_c} < 0. \quad (13)$$

For the other components $j \neq c$, we get

$$\frac{\partial L}{\partial p_j} = -\gamma p_j^{\gamma-1} \log(1 - p_j) + \frac{p_j^\gamma}{1 - p_j} > 0. \quad (14)$$

L_{CECL} supervises the model to increase p_c in the correct class and decrease p_j for $j \neq c$ by minimizing the loss value directly. It teaches the model to learn a single token faster.

However, the backpropagation is performed per batch and the proportion of positive and negative samples in different categories varies from batch to batch. The distribution is also different from the whole dataset. We have done experiments with dynamic loss whose weights are re-calculated per batch. However, it learns not well from it. It may be easier for the model to learn from fixed patterns of mass behavior.

Suppose that the amounts of each category in the dataset are $N_1 : N_2 : \dots : N_C$ and $\sum_{i=1}^C N_i = N$. Furthermore, suppose that all predictions for positive and negative samples in each category are the same to simplify the analysis. We get

$$L = -\frac{1}{N} \sum_{j=1}^C \left(\alpha_j N_j (1 - p_{j,+})^\gamma \log p_{j,+} + \beta_j (N - N_j) p_{j,-}^\gamma \log(1 - p_{j,-}) \right), \quad (15)$$

where $p_{j,+}$ is the prediction for positive samples in class j and $p_{j,-}$ is the prediction for negative samples for class j .

- For categorical cross-entropy L_{CE} ($\boldsymbol{\beta} = \mathbf{0}$, $\boldsymbol{\alpha} = \mathbf{1}$ and $\gamma = 0$ in (15)), solve by Lagrange multiplier under the condition $p_1 + p_2 + \dots + p_C = 1$

$$\frac{\partial L}{\partial p_j} = -\frac{N_j}{N} \frac{1}{p_j} \quad (16)$$

for $j = 1, \dots, C$. If the data is very imbalanced, L_{CE} can not get optimal. For example: If $N_1 = 20N_2$ and N_1 represent the numbers of negative samples, then $p_1 = 20p_2 = 1$ and $p_2 = 0.05$ can't get the correct class when $y_2 = 1$. Thus L_{CE} learns better on the major data.

- For weighted cross-entropy L_{WCE} ($\boldsymbol{\beta} = \mathbf{0}$ and $\gamma = 0$), Lagrange Multiplier gives

$$\frac{\partial L}{\partial p_j} = -\frac{\alpha_j N_j}{N} \frac{1}{p_j}. \quad (17)$$

It concludes that $\boldsymbol{\alpha} = (\frac{N}{N_1}, \dots, \frac{N}{N_c})$ may get the best prediction. It learns more equally accurately in each category.

- For L_{WFCECL} ($\boldsymbol{\beta} \neq \mathbf{0}$ and $\boldsymbol{\alpha} \neq \mathbf{0}$), its gradient is

$$\frac{\partial L}{\partial p_j} = \frac{\partial L}{\partial p_{j,+}} + \frac{\partial L}{\partial p_{j,-}}, \quad (18)$$

where

$$\frac{\partial L}{\partial p_{j,+}} = \alpha_j \frac{N_j}{N} \gamma (1 - p_{j,+})^{\gamma-1} \log p_{j,+} - \alpha_j \frac{N_j}{N} \frac{(1 - p_{j,+})^\gamma}{p_{j,+}} < 0 \quad (19)$$

$$\frac{\partial L}{\partial p_{j,-}} = -\beta_j \frac{N - N_j}{N} \gamma p_{j,-}^{\gamma-1} \log(1 - p_{j,-}) + \beta_j \frac{N - N_j}{N} \frac{p_{j,-}^\gamma}{1 - p_{j,-}} > 0. \quad (20)$$

The gradient from positive samples is negative, making the model increase p_+ . The gradient from negative samples is positive to decrease p_- . Either under standard weights

$$\begin{cases} \boldsymbol{\alpha}_s = (\frac{N-N_1}{N}, \dots, \frac{N-N_C}{N}) \\ \boldsymbol{\beta}_s = (\frac{N_1}{N}, \dots, \frac{N_C}{N}) \end{cases},$$

or EE weights (8), (18) is written as

$$\frac{\partial L}{\partial p_j} = \gamma (1 - p_{j,+})^{\gamma-1} \log p_{j,+} - \frac{(1 - p_{j,+})^\gamma}{p_{j,+}} - \gamma p_{j,-}^{\gamma-1} \log(1 - p_{j,-}) + \frac{p_{j,-}^\gamma}{1 - p_{j,-}} \quad (21)$$

up to scaling. Notice that $\frac{\partial L}{\partial p_j} < 0$ if $p_j < \frac{1}{2}$ and $\frac{\partial L}{\partial p_j} > 0$ if $p_j > \frac{1}{2}$. To enlarge the range of prediction to maintain the gradient negative, we multiply a constant $\lambda \geq 1$ with $\boldsymbol{\alpha}$ in (21). It forces the model to learn from decreasing the loss by contributing larger gradients from positive samples. That is, for $\gamma = 1$, the gradient is

$$\frac{\partial L}{\partial p_j} = \lambda \log p_{j,+} - \lambda \frac{(1 - p_{j,+})}{p_j} - \log(1 - p_{j,-}) + \frac{p_{j,-}}{1 - p_{j,-}}. \quad (22)$$

If $\lambda = 20$, then we get $\frac{\partial L}{\partial p_j} < 0$ for $p_j < 0.831$. Table 9 shows that we do not need large λ and it performs well for $18 \leq \lambda \leq 24$. Experiments are done for $L_{\text{CECLA}_{1,\lambda}}$ loss (7) under batch=8 and 100 epochs.

λ	$\lambda = 1$	$\lambda = 12$	$\lambda = 18$	$\lambda = 20$	$\lambda = 22$	$\lambda = 24$
F ₁	85.1	84.8	85.2	85.7	85.3	85.5
F ₂	86.7	86.8	86.8	87.2	86.9	86.7

Table 9. Multiplication of α

model	CE	WCE	PBP _{0,s}	PBP _{0,1}	PBPA _{0,1}	CL _{0,1}	CLA _{0,1}	CL _{0,s}
category 2	7156	8631	7610	8248	8171	8733	8164	7974
category 3	3887	4426	4386	4459	4647	4386	4407	4234
Macro F ₁	79.9	79.8	79.4	79.1	78.7	79.5	79.4	79.3
Macro F ₂	79.8	83.6	81.5	82.3	82.5	82.6	83.3	81.9

Table 10. Amount and Accuracy Comparison at 50 epochs part 2

model	FCE	FWCE	PBP _{0,8}	PBPA _{0,8}	CL _{1,1}	CLA _{1,1}	CL _{1,20}	CLA _{1,20}
category 2	7198	9161	8375	8218	8405	8626	8885	8564
category 3	4039	4570	4406	4458	4575	4578	4572	4568
Macro F ₁	79.8	79.8	79.9	79.5	78.6	79.4	79.1	79.4
Macro F ₂	80.3	79.3	83.3	82.8	82.5	83.7	83.7	83.5

Table 11. Amount and Accuracy Comparison at 50 epochs part 2

model	CE	WCE	PBP _{0,s}	PBP _{0,1}	PBPA _{0,1}	CL _{0,1}	CLA _{0,1}	CL _{0,s}
category 2	7352	8352	8035	8049	8421	7715	7995	8111
category 3	3915	4071	3894	4133	4133	4112	4138	4287
Macro F ₁	79.8	79.9	79.3	79.1	79.0	79.2	78.8	79.3
Macro F ₂	80.1	82.3	80.6	81.4	81.3	80.7	82.0	82.0

Table 12. Amount and Accuracy Comparison at 100 Epochs Part 1

model	FCE	FWCE	PBP _{0,8}	PBPA _{0,8}	CL _{1,1}	CLA _{1,1}	CL _{1,20}	CLA _{1,20}
category 2	7371	8031	8495	8022	8655	8148	8618	8446
category 3	3735	4111	4065	4240	4301	4296	4258	4124
Macro F ₁	79.7	79.5	79.4	79.3	78.9	79.2	79.0	79.9
Macro F ₂	79.4	81.2	81.9	81.3	82.4	81.8	82.2	82.5

Table 13. Amount and Accuracy Comparison at 100 Epochs Part 2

A.2 Accuracy Comparison of Loss Functions

Table 10, 11, 12 and 13 show the accuracy comparison and category amount prediction of loss functions at 50 and 100 epochs respectively by excluding the category of none. $CL_{1,20}$ represents WCECL loss with EE weight, focal factor $\gamma = 1$ and multiplication factor $\lambda = 20$. $CLA_{1,20}$ represents WCECL loss with array weight, focal factor $\gamma = 1$ and multiplication factor $\lambda = 20$. $PBP_{0,s}$ notes for PBP loss with standard weight and $\gamma = 0$.

L_{CE} and $L_{PBP_{0.8}}$ both obtain the highest F_1 scores at 50 epochs. However, $L_{PBP_{0.8}}$ loss has a much higher F_2 . Category 2 and Category 3 represent keywords in our data. Since $L_{PBP_{0.8}}$ returns more results, it is more competitive in keyword extraction. In Figure 4, L_{CE} underestimates category amount prediction. It has higher precision and lower recall (higher F_1 and lower F_2 shown in Table 10, 11, 12, and 13). It is not beneficial for auto-tagging. A direct computation gives that

$$F_1 - F_2 = \frac{3pr(p-r)}{(p+r)(4p+r)}.$$

This formula shows the tradeoff between precision-recall and $F_1 - F_2$.

The dot pink horizontal line represents the true amount of category in Figure 4 and 5. $L_{CLA_{1,20}}$, $L_{PBP_{0.8}}$, and L_{WCE} return more labels of keywords. Besides, they maintain almost the same F_1 as L_{CE} but much higher F_2 . These new objective functions return not only more truly relevant but also more accurate results.

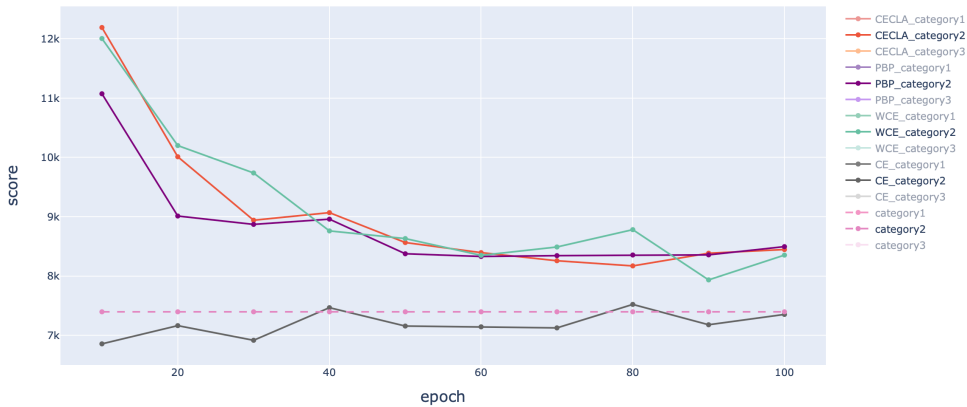


Fig. 4. Amount Prediction for Category 2

L_{CECL} performs better with array weights at 100 epochs. L_{PBP} learn better with EE weights at 50 epochs. L_{CECL} has more portion with EE weight than standard weight on

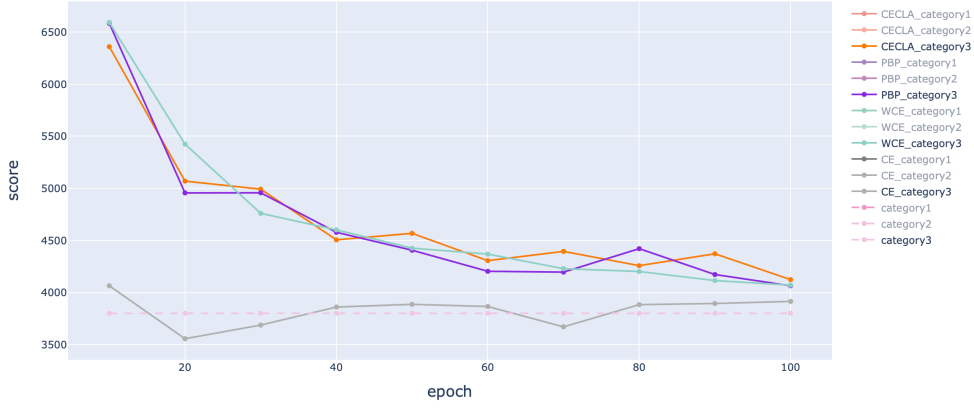


Fig. 5. Amount Prediction for Category 3

the microdata and it has less prediction on the counts at 100 epochs. Since the negative samples of L_{CECLA} depend on categories, it predicts more counts than EE weight on the microdata at 100 epochs. See the following section for an explanation.

A.2.1 EE Weights vs Standard Weights for CECL Loss Suppose that $N_i < N_j < N - N_j < N - N_i$. That is, the data in class i is more imbalanced than in class j . Recall the EE weights

$$\begin{cases} \alpha_{EE} = \left(\frac{N}{N_1}, \dots, \frac{N}{N_C} \right) \\ \beta_{EE} = \left(\frac{N}{(N-N_1)}, \dots, \frac{N}{(N-N_C)} \right) \end{cases},$$

and standard weights

$$\begin{cases} \alpha_{st} = \left(\frac{N-N_1}{N}, \dots, \frac{N-N_C}{N} \right) \\ \beta_{st} = \left(\frac{N_1}{N}, \dots, \frac{N_C}{N} \right) \end{cases}.$$

The proportion of the positive and negative weight is the same

$$(\alpha_{EE,i} : \beta_{EE,i}) = \frac{N}{(N - N_i)N_i} (\alpha_{st,i} : \beta_{st,i}).$$

Although the proportion $\alpha_i : \beta_i$ is the same, $\frac{N}{N_i(N-N_i)} > \frac{N}{N_j(N-N_j)}$ reveals that a single token from micro data gets more punishment than major data. The model predicts more category amounts for microdata with EE weights than standard weights in the early stage but the other around at 100 epochs. EE weights obtain less F_1 scores but higher F_2 scores.

A.3 Comparison of WCE, CECLA, and PBP Loss

The differences between L_{WCE} , L_{CECLA} , and L_{PBP} :

- For contrastive learning type of functions (with β), their gradient (18) has more bounce back between positive and negative samples. Its F scores also have more up and down. It has a better chance to obtain the optimal point. From Figure 6, L_{CECLA} achieves best macro F₂ score at 40 epochs. On the other hand, L_{WCE} only has the contribution from positive samples. Its F scores curves are steadily increasing or decreasing. It requires a longer time to achieve the optimal.
- In general, L_{PBP} converges faster than other loss functions. It has a higher F₁ than L_{WCE} along with training. At 40 epochs, L_{PBP} performs better than L_{WCE} .

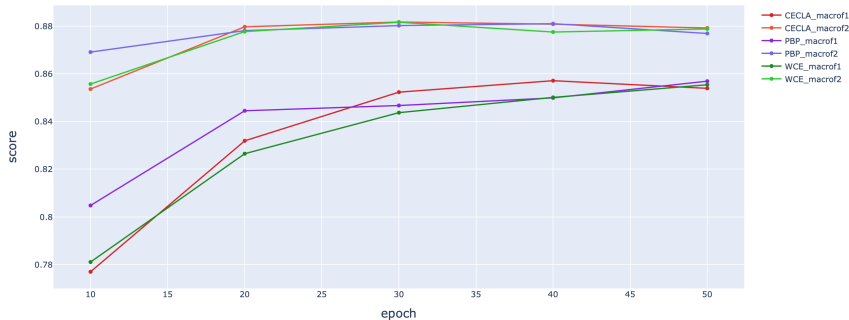


Fig. 6. CECLA vs PBP vs WCE

B Experiment Setup

The source codes of SOTA models are obtained either from their official or third trustable Github.

- Admin: <https://github.com/LiyuanLucasLiu/Transformer-Clinic>
- Muse: <https://github.com/lancopku/Prime>
- Performers: https://github.com/google-research/google-research/tree/master/performer/fast_attention/tensorflow/fast_attention.py
- Transformer: <https://www.tensorflow.org/text/tutorials/>
- Informer: <https://github.com/zhouhaoyi/Informer2020>
- Switch: https://keras.io/examples/nlp/text_classification_with_switch_transformer/

B.1 Setup for Deeper Layers

We set `warmup_steps = 8000` in (10) for 12 and 24-layer structures of all SOTA models. They adapt `lr/3` for their 12-layer structure. This reduces the slope for the warmup stage smaller than it in (10).

- BAT changes the learning rate to `lr/5` for its 24-layer structure to a finer convergence.
- We finalize `warmup_steps = 12000` and `lr/10` for the 24-layer structure of Transformer. However, its convergence is not satisfying after several tries.
- The learning rate for the 24-layer structure of MUSE, Performers, and Informer maintains `lr/3`.
- Since the average tokens in EC-Zh is 46.6. We select the expert numbers $E = 50$ and capacity $C = 1$ for Switch. Its learning rate is converted to `lr/10` for its 24-layer structure. A model with a large number of parameters needs a smaller learning rate to converge.

References

1. R. Campos, V. Mangaravite, A. Pasquali, A. M. Jorge, C. Nunes, and A. Jatowt. Yake! In *Advances in Information Retrieval - 40th European Conference on IR Research, ECIR 2018, Grenoble, France, March 26-29, 2018, Proceedings*, volume 10772 of *Lecture Notes in Computer Science*, pages 806–810. Springer, 2018.
2. K. Cho, B. van Merriënboer, D. Bahdanau, and Y. Bengio. On the properties of neural machine translation: Encoder-decoder approaches. In *Proceedings of SSST@EMNLP 2014, Eighth Workshop on Syntax, Semantics and Structure in Statistical Translation, Doha, Qatar, 25 October 2014*, pages 103–111. Association for Computational Linguistics, 2014.
3. K. Choromanski, V. Likhoshesterov, D. Dohan, X. Song, A. Gane, T. Sarlós, P. Hawkins, J. Davis, A. Mohiuddin, L. Kaiser, D. Belanger, L. Colwell, and A. Weller. Rethinking attention with performers, 2020.
4. W. Fedus, B. Zoph, and N. Shazeer. Switch transformers: Scaling to trillion parameter models with simple and efficient sparsity, 2021.
5. R. Hadsell, S. Chopra, and Y. LeCun. Dimensionality reduction by learning an invariant mapping. In *2006 IEEE Computer Society Conference on Computer Vision and Pattern Recognition (CVPR 2006), 17-22 June 2006, New York, NY, USA*, pages 1735–1742. IEEE Computer Society, 2006.
6. P. Huang, X. He, J. Gao, L. Deng, A. Acero, and L. P. Heck. Learning deep structured semantic models for web search using clickthrough data. In Q. He, A. Iyengar, W. Nejdl, J. Pei, and R. Rastogi, editors, *22nd ACM International Conference on Information and Knowledge Management, CIKM'13, San Francisco, CA, USA, October 27 - November 1, 2013*, pages 2333–2338. ACM, 2013.
7. D. P. Kingma and J. Ba. Adam: A method for stochastic optimization. In Y. Bengio and Y. LeCun, editors, *3rd International Conference on Learning Representations, ICLR 2015, San Diego, CA, USA, May 7-9, 2015, Conference Track Proceedings*, 2015.
8. L. Liu, X. Liu, J. Gao, W. Chen, and J. Han. Understanding the difficulty of training transformers. In *Proceedings of the 2020 Conference on Empirical Methods in Natural Language Processing, EMNLP 2020, Online, November 16-20, 2020*, pages 5747–5763. Association for Computational Linguistics, 2020.
9. R. Mihalcea and P. Tarau. TextRank: Bringing order into texts. In *Proceedings of EMNLP-04 and the 2004 Conference on Empirical Methods in Natural Language Processing*, July 2004.
10. R. Nogueira and K. Cho. Passage re-ranking with BERT, 2019.
11. A. Radford, K. Narasimhan, T. Salimans, and I. Sutskever. Improving language understanding with unsupervised learning. <https://openai.com/blog/language-unsupervised/>, 2018.
12. S. Rose, D. Engel, N. Cramer, and W. Cowley. Automatic keyword extraction from individual documents. In M. W. Berry and J. Kogan, editors, *Text Mining. Applications and Theory*, pages 1–20. John Wiley and Sons, Ltd, 2010.
13. F. Schroff, D. Kalenichenko, and J. Philbin. Facenet: A unified embedding for face recognition and clustering. In *IEEE Conference on Computer Vision and Pattern Recognition, CVPR 2015, Boston, MA, USA, June 7-12, 2015*, pages 815–823. IEEE Computer Society, 2015.

14. D. R. So, C. Liang, and Q. V. Le. The evolved transformer. In *Proceedings of the 36th International Conference on Machine Learning, ICML 2019, 9-15 June 2019, Long Beach, California, USA*, volume 97 of *Proceedings of Machine Learning Research*, pages 5877–5886. PMLR, 2019.
15. K. Sohn. Improved deep metric learning with multi-class n-pair loss objective. In *Advances in Neural Information Processing Systems 29: Annual Conference on Neural Information Processing Systems 2016, December 5-10, 2016, Barcelona, Spain*, pages 1849–1857, 2016.
16. M. Tang, P. Gandhi, M. A. Kabir, C. Zou, J. Blakey, and X. Luo. Progress notes classification and keyword extraction using attention-based deep learning models with BERT, 2019.
17. A. Vaswani, N. Shazeer, N. Parmar, J. Uszkoreit, L. Jones, A. N. Gomez, L. Kaiser, and I. Polosukhin. Attention is all you need. In *Advances in Neural Information Processing Systems*, volume 30. Curran Associates, Inc., 2017.
18. X. Wan and J. Xiao. Collabrank: Towards a collaborative approach to single-document keyphrase extraction. In D. Scott and H. Uszkoreit, editors, *COLING 2008, 22nd International Conference on Computational Linguistics, Proceedings of the Conference, 18-22 August 2008, Manchester, UK*, pages 969–976, 2008.
19. C. Xiong, Z. Dai, J. Callan, Z. Liu, and R. Power. End-to-end neural ad-hoc ranking with kernel pooling. In *Proceedings of the 40th International ACM SIGIR Conference on Research and Development in Information Retrieval, Shinjuku, Tokyo, Japan, August 7-11, 2017*, pages 55–64. ACM, 2017.
20. Z. Yang, Q. Lan, J. Guo, Y. Fan, X. Zhu, Y. Lan, Y. Wang, and X. Cheng. A deep top-k relevance matching model for ad-hoc retrieval. In *Information Retrieval - 24th China Conference, CCIR 2018, Guilin, China, September 27-29, 2018, Proceedings*, volume 11168 of *Lecture Notes in Computer Science*, pages 16–27. Springer, 2018.
21. Q. Zhang, Y. Wang, Y. Gong, and X. Huang. Keyphrase extraction using deep recurrent neural networks on twitter. In J. Su, X. Carreras, and K. Duh, editors, *Proceedings of the 2016 Conference on Empirical Methods in Natural Language Processing, EMNLP 2016, Austin, Texas, USA, November 1-4, 2016*, pages 836–845. The Association for Computational Linguistics, 2016.
22. G. Zhao, X. Sun, J. Xu, Z. Zhang, and L. Luo. MUSE: parallel multi-scale attention for sequence to sequence learning, 2019.
23. H. Zhou, S. Zhang, J. Peng, S. Zhang, J. Li, H. Xiong, and W. Zhang. Informer: Beyond efficient transformer for long sequence time-series forecasting, 2020.